CodY Activates Transcription of a Small RNA in *Bacillus subtilis*[▽][†]

Heike Preis, Rita A. Eckart, Rajani K. Gudipati,[‡] Nadja Heidrich,[§] and Sabine Brantl*

Friedrich-Schiller-Universität Jena, Biologisch-Pharmazeutische Fakultät, AG Bakteriengenetik, Philosophenweg 12, Jena D-07743, Germany

Regulatory small RNAs (sRNAs) in bacterial genomes have become a focus of research over the past 8 years. Whereas more than 100 such sRNAs have been found in *Escherichia coli*, relatively little is known about sRNAs in gram-positive bacteria. Using a computational approach, we identified two sRNAs in intergenic regions of the *Bacillus subtilis* genome, SR1 and SR2 (renamed BsrF). Recently, we demonstrated that SR1 inhibits the translation initiation of the transcriptional activator AhrC. Here, we describe detection of BsrF, its expression profile, and its regulation by CodY. Furthermore, we mapped the secondary structure of BsrF. BsrF is expressed in complex and minimal media in all growth phases in *B. subtilis* and, with a similar expression profile, also in *Bacillus amyloliquefaciens*. Neither overexpression nor deletion of *bsrF* affected the growth of *B. subtilis*. BsrF was found to be long-lived in complex and minimal media. Analysis of 13 putative transcription factor binding sites upstream of *bsrF* revealed only an effect for CodY. Here, we showed by using Northern blotting, *lacZ* reporter gene fusions, in vitro transcription, and DNase I footprinting that the transcription of *bsrF* is activated by CodY in the presence of branched-chain amino acids and GTP. Furthermore, BsrF transcription was increased 1.5- to 2-fold by glucose in the presence of branched-chain amino acids, and this increase was independent of the known glucose-dependent regulators. BsrF is the second target for which transcriptional activation by CodY has been discovered.

Bacterial small RNAs (sRNAs) play important roles as stress regulators in metabolic processes (for a review, see reference 42) or virulence gene regulators (for a review, see reference 45). Over the past 8 years, more than 100 sRNAs have been discovered in *Escherichia coli*, and it is estimated that 200 to 300 such RNAs are present in an average bacterial genome (19). We distinguish base-pairing sRNAs (antisense RNAs) and sRNAs that act by protein binding (for a review, see reference 5). Many *trans*-encoded antisense RNAs have multiple targets. The majority of them block translation initiation, whereas others affect the stability of their target mRNAs (for a review, see reference 5).

Meanwhile, a few systematic searches have been performed for gram-positive bacteria. In *Bacillus subtilis*, 24 sRNAs are known (1, 24, 35, 39, 40), and targets for 5 of them have been identified; RatA controls the toxin TxpA (39), SR1 controls the transcription activator AhrC (17) (see below), FsrA regulates *sdhCAB*, *citB*, *yvfW*, and *leuCD* (11), and BsrA and BsrB are two 6S RNAs (1). In *Staphylococcus aureus*, in addition to RNAIII (3), 12 novel sRNAs from pathogenicity islands have been detected (33). Furthermore, in *Listeria monocytogenes*, three Hfq-binding sRNAs with unknown functions (8) and nine novel sRNAs in intergenic regions have been identified (27). In 2007, five sRNAs controlled by the response regulator

CiaR were found in *Streptococcus pneumoniae* (14). However, identification of mRNA targets of the previously discovered bacterial sRNAs is rather difficult and has been successful in only a few cases. Recently, all currently known chromosome-encoded sRNAs for which targets have been identified were summarized (5).

The majority of sRNAs from *E. coli* bind the abundant RNA chaperone Hfq (47, 49). Thus, Hfq is required for stabilization of the sRNAs and/or to promote complex formation with the target RNAs. However, for sRNAs from gram-positive bacteria, the putative function of Hfq is still elusive (5).

Recently, we have demonstrated that SR1, which was found by using a computational approach and subsequent Northern blotting (24), acts by base pairing with its primary target, *ahrC* mRNA encoding the transcriptional activator of the *rocABC* and *rocDEF* arginine catabolic operons (17). Seven complementary regions between SR1 and *ahrC* were identified, and the most 5′ region, region G, is located 97 nucleotides (nt) downstream from the *ahrC* ribosome binding site. SR1 inhibits translation initiation of *ahrC* mRNA by a novel mechanism: induction of structural changes downstream from the ribosome binding site (18). Interestingly, SR1 is expressed under gluconeogenic conditions and repressed under glycolytic conditions, and the repression is mediated mainly by CcpN and, to a minor extent, by CcpA (24, 25).

CodY was first identified as a repressor of the *B. subtilis* dipeptide permease (*dppABCDE*) operon and turned out to be a critical regulator in the control of the expression of stationary-phase genes and the initiation of sporulation. Meanwhile, it has been found that CodY regulates more than 100 genes in *B. subtilis*, the products of which are involved in adaptation to poor growth conditions (for a review, see reference 41). CodY homologues have been found to be encoded in almost all low-G+C-content gram-positive bacteria, including six *Bacillus* species and eight *Streptococcus* species, and in some cases they

* Corresponding author. Mailing address: Friedrich-Schiller-Universität Jena, Biologisch-Pharmazeutische Fakultät, AG Bakteriengenetik, Philosophenweg 12, Jena D-07743, Germany. Phone: 49-3641-949570. E-mail: Sabine.Brantl@uni-jena.de.
‡ Present address: Centre de Génétique Moléculaire, CNRS, Gif sur Yvette, France.
§ Present address: Department of Cell and Molecular Biology, Biomedical Center, Uppsala University, Box 596, S-75124 Uppsala, Sweden.

have been purified (41). CodY appears to play the global role in *B. subtilis* and its relatives that Lrp plays in gram-negative bacteria, but it has an even broader role as it regulates anabolic, catabolic, differentiation, and virulence pathways. In the majority of cases, CodY acts as a transcriptional repressor in the logarithmic growth phase. It has been demonstrated that *B. subtilis* CodY binds two ligands, GTP (34) and branched-chain amino acids (BCAA) (37), which, to different extents, increase the repression activity of CodY. So far, the *B. subtilis* acetate kinase (*ackA*) gene is the only known gene for which CodY (in concert with CcpA) acts as a transcriptional activator (38).

Here, we report the properties of a novel sRNA, SR2 (30), in *B. subtilis*. SR2 was found by our group by using a combination of computational search and Northern blotting that previously also identified SR1. Recently, SR2 was also found using an independent approach by Saito et al. and was designated BsrF (35). Therefore, we use the designation BsrF below. BsrF is expressed in complex and minimal media from early logarithmic to late stationary growth, but the expression decreases when cells start to sporulate. Neither overexpression nor deletion of *bsrF* affected the growth of *B. subtilis*. Interestingly, the *bsrF* gene is also expressed in *Bacillus amyloliquefaciens*. Half-life measurements showed that BsrF is very stable. Secondary structure probing of BsrF identified a branched stem-loop structure and the transcription terminator. Of 13 transcription factors for which hypothetical binding sites were found upstream of *bsrF*, only CodY proved to have an effect. We demonstrate here that in the presence of BCAA, CodY activates *bsrF* transcription by binding 329 bp upstream of the *bsrF* transcription start site. Consequently, *bsrF* is the second gene for which an activating effect of CodY has been found. Furthermore, in the presence of BCAA, glucose activated BsrF transcription 1.5- to 2-fold, and this activation was independent of CcpA, CcpN, CcpC, GlcR, and CggR.

MATERIALS AND METHODS

Enzymes and chemicals. The chemicals used were the highest purity available. *Taq* DNA polymerase was purchased from Roche, and Firepol polymerase was purchased from Solis Biodyne, Estonia. DNase I was purchased from Ambion, and the Thermoscript reverse transcription system was purchased from Invitrogen.

Strains, media, and growth conditions. *E. coli* strain DH5α, *B. subtilis* strains DB104 (21), PS251 (*codY*::(*erm*::*spc*) *trpC2* (2), and QB5407 (*ccpA*::*spc*) (10), and *B. amyloliquefaciens* FZB42 were used. TY medium was used as a complex medium for *E. coli* and *Bacillus* (17). Spizizen and CSE media were used as minimal media for *B. subtilis* (17). SP medium (8 g nutrient broth, 0.25 g MgSO$_4$ · 7 H$_2$O, 1 g KCl, 1 ml CaCl$_2$ [0.5 M], 1 ml MnCl$_2$ [10 mM], and 2 ml ammonium iron citrate [2.2 mg/ml] dissolved in 1 liter) was used as the sporulation medium.

Isolation of chromosomal DNA from *B. subtilis*. Chromosomal DNA was isolated from *B. subtilis* strains as described previously (24).

Primer extension. Primer extension experiments were carried out as described previously (24) using total RNA from *B. subtilis* strain DB104 and 5′-labeled oligodeoxyribonucleotide SB847.

Construction of plasmids for *bsrF* knockout and overexpression strains. To obtain a *bsrF* knockout strain, plasmid pINT5 was constructed in the following way. First, DNA fragments upstream and downstream from the *bsrF* gene were amplified by PCR using chromosomal DNA of *B. subtilis* DB104 and oligodeoxyribonucleotides SB813 (see Table S1 in the supplemental material) and SB814, as well as oligodeoxyribonucleotides SB815 and SB816, and, after digestion with the appropriate restriction enzymes, were inserted as BamHI/EcoRI or SalGI/PstI fragments into the corresponding pUC19 vectors cleaved with the same pair of enzymes. This approach resulted in pFRONT5 and pBACK5. Next, plasmid pCBACK5 was constructed by jointly cloning the CAT-EcoRI/SalI fragment of vector pCAT (24) and the BACK-SalGI/PstI fragment of vector

pBACK5 into the pUC19 EcoRI/PstI vector. Subsequently, the EcoRI/PstI fragment of pCBACK was jointly cloned with the BamHI/EcoRI fragment of pFRONT5 into the pUC19 BamHI/PstI vector, resulting in integration vector pINT5. All fragments were confirmed by sequencing.

Plasmid pWSR2, which was used for inducible overexpression of *bsrF* in *B. subtilis*, was constructed as follows. The promoterless *bsrF* gene was amplified with oligodeoxyribonucleotides SB1063 and SB1064 using chromosomal DNA of *B. subtilis* DB104 as the template, digested with HindIII, and inserted into the pUC19 HindIII-vector, resulting in plasmid pUCSR2. The insert was confirmed by sequencing. Subsequently, the pUCSR2 HindIII fragment was inserted into the unique HindIII site of vector pWH353 (12) downstream of the *tet* promoter, yielding plasmid pWSR2, and the correct insert orientation was verified by sequencing. Plasmid pUCBSR2, which was used for constitutive overexpression of *bsrF* in *B. subtilis* under its own promoter, was obtained by cloning a BamHI/HindIII fragment obtained by performing PCR with chromosomal DNA and primers SB832 and SB833 into the BamHI/HindIII-digested vector pUCB2.

Construction of plasmids for transcriptional *lacZ* fusions and determination of β-galactosidase activity. To construct plasmid pACG6 containing the largest *bsrF-lacZ* transcriptional fusion (415 bp upstream of *bsrF* transcriptional start site), a PCR was performed with chromosomal DNA of strain DB104 and oligodeoxyribonucleotides SB1233 and SB868. The resulting fragment was digested with EcoRI and BamHI and inserted into the pAC6 (43) vector cleaved with the same enzymes. All other pACG derivatives comprising progressively shorter upstream regions were constructed in the same way and are listed in Table 1.

Transcriptional fusions containing mutations in the CodY binding site were obtained by using a two-step PCR as described below for pACG11. First, two PCRs with primer pairs SB1233/SB1260 and SB1259/SB868 were carried out, and subsequently, the joined, gel-purified fragments were subjected to a second PCR with outer primers SB1233 and SB868. The resulting fragment was digested with EcoRI and BamHI and inserted into the EcoRI/BamHI-digested pAC6 vector. The other *codY* mutant pAC6 derivatives pACG15, pACG18, and pACG19 (Table 1) were constructed in the same way. All pAC6 derivatives were linearized with ScaI and inserted into the *amyE* locus of the *B. subtilis* DB104 chromosome by double crossing over. The resulting integrant strains were used for determination of β-galactosidase activities as described previously (4).

Preparation of total RNA, RNA gel electrophoresis, and Northern blotting. Preparation of total RNA, RNA gel electrophoresis on 1.5% agarose gels and 6% denaturing polyacrylamide gels, and Northern blotting were carried out as described previously (17).

Purification of CodY and DNase I footprinting. C-terminally six-histidine-tagged CodY was purified from *E. coli* overexpression strain KS272(pKT1) as described previously (22). DNase I footprinting was performed as described previously (25). GTP and each of the BCAA isoleucine, leucine, and valine were added prior to DNase I at final concentrations of 2 mM and 10 mM, respectively. Both a PCR fragment obtained with primers SB1233 and SB868 and a fragment obtained by annealing of oligodeoxyribonucleotide SB1306 and SB1307 were used for DNase I treatment.

In vitro transcription with *B. subtilis* RNA polymerase. In vitro transcription with purified *B. subtilis* RNA polymerase was performed as described previously (6). Dried gels were analyzed and subjected to phosphorimaging (Fujix BAS 1000).

In vitro transcription with T7 RNA polymerase and RNA secondary structure probing. In vitro transcription with T7 RNA polymerase and partial digestion of in vitro-synthesized, 5′-end-labeled BsrF with RNases T$_1$, T$_2$, and V were carried out as described previously (16).

RESULTS

A combination of computer prediction and Northern blotting identified the novel sRNA SR2 (BsrF) in an intergenic region of the *B. subtilis* genome. Previously, we used a computational approach to predict noncoding sRNAs in intergenic regions of the *B. subtilis* genome (24). Briefly, all potential transcription terminators in the *B. subtilis* genome were predicted, and subsequently, 50 to 450 bp upstream of these terminators promoters were predicted based on both consensus promoter sequences and data in the DTBS promoter database. Finally, all predicted sequences were evaluated by using different criteria (24), which yielded 25 candidate sRNAs. Oligo-

TABLE 1. Plasmids used in this study

Plasmid	Description	Reference
pUC19	*E. coli* cloning vector, Ap[r], multiple cloning site	36
pUCB2	Shuttle vector for pUC19 and pUB110, Km[r] Pm[r]	Brantl, unpublished data
pCAT	pUC19 with 1.4-kb CAT gene	24
pAC6	Vector for integration of transcriptional *lacZ* fusions	42
pWH353	*E. coli-B. subtilis* shuttle vector, Tet system, Km[r]	12
pWSR2	pWH353 with *bsrF* gene under *tet*-inducible promoter	This study
pUCBSR2	pUCB2 with *bsrF* gene under its own promoter	This study
pFRONT5	pUC19 with 800 bp upstream of *bsrF*	This study
pBACK5	pUC19 with 500 bp downstream of *bsrF*	This study
pCBACK5	pBACK5 with CAT gene from pCAT	This study
pINT5	Vector for replacement of *bsrF* by CAT gene	This study
pACG6	pAC6 with 415 bp upstream of *bsrF* transcription start site	This study
pACG9	pAC6 with 375 bp upstream of *bsrF* transcription start site	This study
pACG10	pAC6 with 302 bp upstream of *bsrF* transcription start site	This study
pACG12	pAC6 with 71 bp upstream of *bsrF* transcription start site	This study
pACG13	pAC6 with 89 bp upstream of *bsrF* transcription start site	This study
pACG16	pAC6 with 58 bp upstream of *bsrF* transcription start site	This study
pACG17	pAC6 with 48 bp upstream of *bsrF* transcription start site	This study
pACG4	pACG6 with 35 bp upstream of *bsrF* transcription start site	This study
pACG11	pACG6 with two point mutations in CodY binding site	This study
pACG15	pACG6 with one point mutation in CodY binding site	This study
pACG18	pACG6 with two point mutations in CodY binding site	This study
pACG19	pACG6 with two point mutations in CodY binding site	This study

nucleotides were designed to confirm these RNAs in Northern blots. Using this approach, two novel sRNAs were discovered, which were designated SR1 (sRNA 1) and SR2 (sRNA 2; now BsrF). SR1 (205 nt) was described previously (24) and subsequently was characterized in some detail (17, 18). BsrF was

found later and is approximately 110 nt long (see below). The *bsrF* gene is located in the intergenic region between the uncharacterized gene *yobO* and *csaA* (Fig. 1A). The *bsrF* gene and *csaA* overlap by 30 bp in their terminator regions (Fig. 1). The *bsrF* promoter is a typical σ[A] promoter and comprises −35
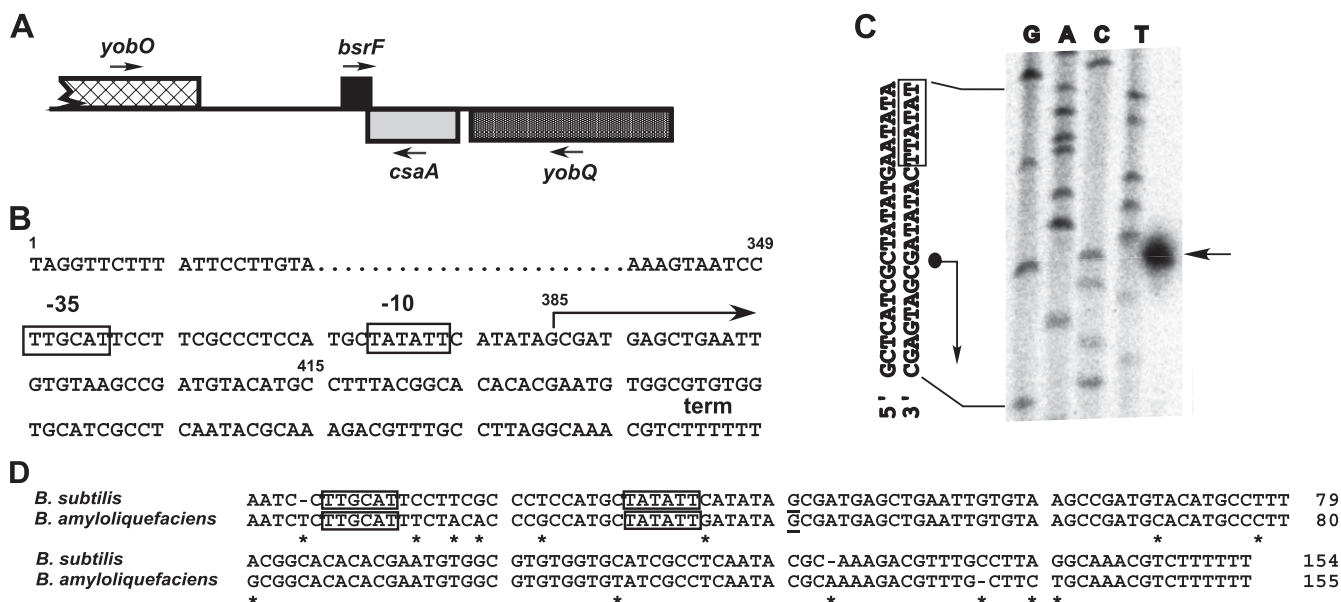

FIG. 1. Location of the *bsrF* gene. (A) Schematic diagram of the location of the *bsrF* gene on the *B. subtilis* chromosome. The direction of transcription is indicated by arrows. Genes transcribed from the plus strand are indicated above the line. (B) Sequence of the *bsrF* gene. −35 and −10 boxes of the *bsrF* promoter are indicated. The start site and direction of transcription are indicated by an arrow, and the transcription termination site is indicated by term. The transcription start site is at position 2078305 in the *B. subtilis* genome. The small numbers indicate the positions of nucleotides referred to in Fig. 8. (C) Mapping of the 5′ end of BsrF. The results of a sequencing reaction with pUCBSR2 (containing the entire *bsrF* gene under its own promoter) and primer SB847 are shown in the left four lanes. The lane on the right shows the results of a primer extension reaction with total RNA of *B. subtilis* DB104 and 5′-labeled primer SB847. The arrow indicates the transcriptional start site of BsrF. Part of the sequence is shown on the left. The dot and the arrow indicate the mapped transcriptional start site. (D) Alignment of the *bsrF* genes of *B. subtilis* and *B. amyloliquefaciens*. Promoter boxes are indicated by boxes, and the transcription start site is underlined.
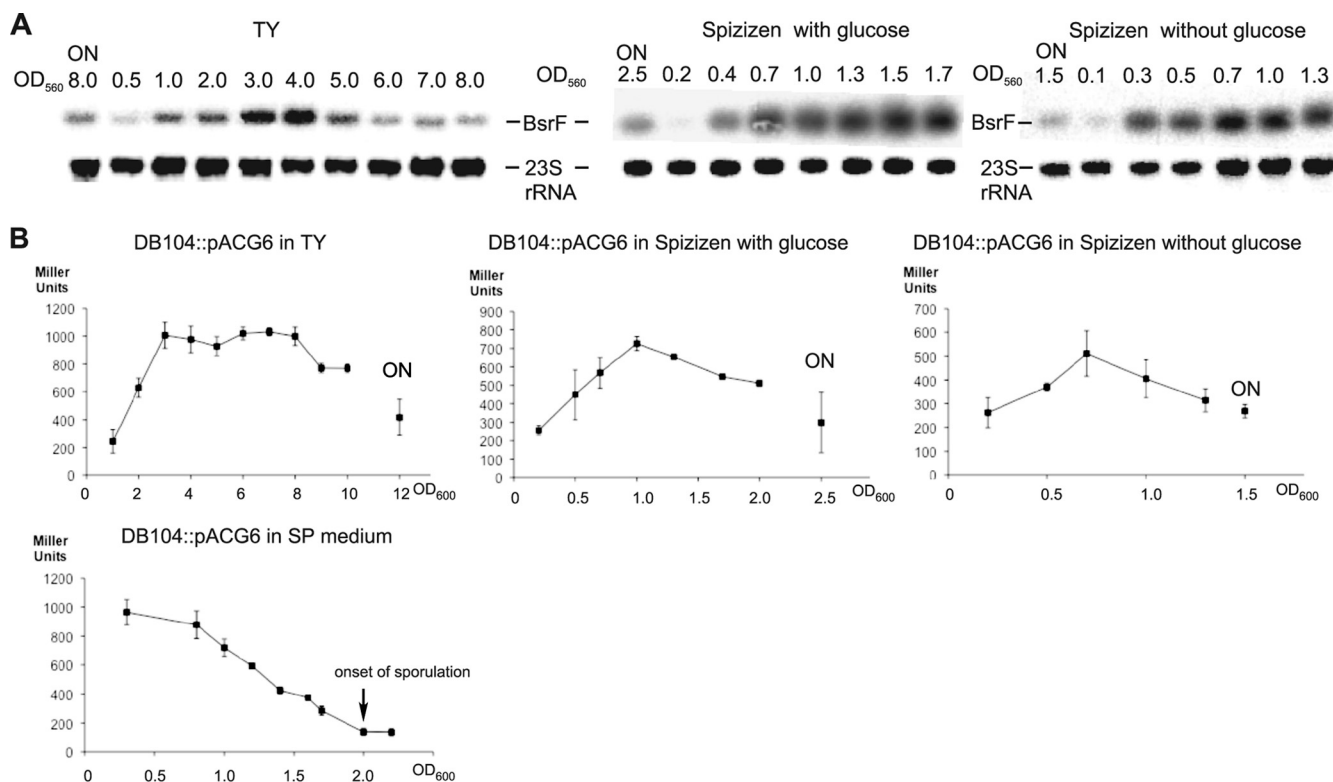
FIG. 2. Expression profile of BsrF. (A) Expression of BsrF in complex and minimal media as monitored by Northern blotting. *B. subtilis* strain DB104 was grown in different media, and aliquots were removed at the OD_{560} indicated, immediately frozen in liquid nitrogen, and later used for preparation of total RNA. RNA was treated with glyoxal, separated on 2% agarose gels, blotted onto a nylon membrane, and hybridized with an [α-^{32}P]dATP-labeled BsrF-specific DNA probe. Autoradiograms of the corresponding gels are shown. ON, overnight cultivation (~15 h). For correction of loading errors, filters were reprobed with [γ-^{32}P]ATP-labeled oligonucleotide SB747 specific for 23S rRNA. (B) Expression of BsrF in complex, minimal, and sporulation media as monitored by measurement of the β-galactosidase activity. *B. subtilis* strain DB104::pACG6 was grown in different media, and at the OD_{600} indicated, samples were withdrawn and used for measurement of the β-galactosidase activity. The data are the averages ± standard deviations for three independent measurements. ON, overnight cultivation.

and −10 boxes that are close to the consensus and separated by a 17-bp GC-rich spacer (Fig. 1B). As shown in Fig. 1C, the 5′ end of BsrF was mapped. A search for potential open reading frames (ORFs) in the BsrF gene revealed an ORF consisting of 24 codons. However, this ORF lacks an appropriately located Shine-Delgarno sequence, and no homolog of its deduced protein product was found in the GenBank database. Therefore, BsrF is probably a noncoding sRNA. A search for BsrF homologues in other gram-positive bacteria yielded results only for *B. amyloliquefaciens* (Fig. 1D).

BsrF is expressed in complex and minimal media throughout growth, but the expression decreases when cells start to sporulate. To investigate the expression profile of BsrF, strain DB104 was grown at 37°C in either complex TY or Spizizen minimal medium with or without glucose, and total RNA having different optical densities was prepared and subjected to Northern blotting. As shown in Fig. 2A, the level of expression of BsrF is very low in the early logarithmic growth phase, increases at the end of the logarithmic growth phase, remains high during stationary phase, and decreases slightly at late stationary phase. Even after overnight cultivation (late stationary phase), BsrF is significantly expressed in all three media. These data were substantiated by measurement of β-galactosidase activity using all three media from early logarithmic

phase until late stationary phase and plasmid pACG6 comprising a transcriptional *bsrF-lacZ* fusion with 415 bp upstream of the transcription start site, which was integrated into the *amyE* locus of strain DB104 (Fig. 2B). To analyze the effect of sporulation on *bsrF* expression, DB104::pACG6 was cultivated in SP sporulation medium for 15 h. The β-galactosidase activities showed that BsrF transcription decreases progressively when cells start to sporulate and, after 15 h, is about one-eighth the initial value (Fig. 2B).

Neither *bsrF* knockout nor overexpression affect the growth of *B. subtilis*. To find out whether BsrF is essential in *B. subtilis*, a *bsrF* knockout strain was constructed. Vector pINT5 carrying the CAT gene flanked by the upstream and downstream regions of the *bsrF* wild-type gene was constructed as described in Materials and Methods and integrated into the chromosome of *B. subtilis* DB104. Successful integration by double crossing over was confirmed by PCR and Northern blotting. The growth curves of the Δ*bsrF* strain grown in TY medium and in minimal medium with or without glucose at 37°C were identical to the growth curves of the wild-type strain (see Fig. S1 in the supplemental material).

To analyze whether overexpression of *bsrF* has significant physiological effects, two overexpression strains were constructed, one for inducible overexpression under control of the
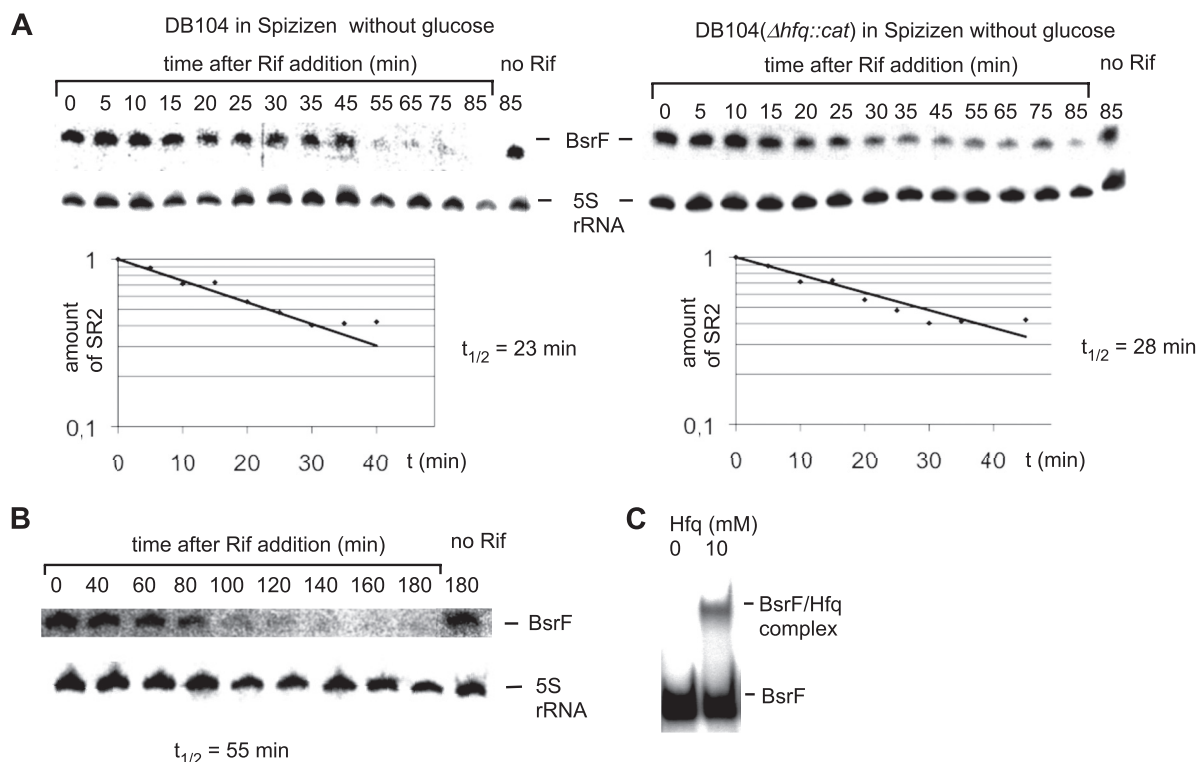
FIG. 3. Determination of the BsrF half-lives in different media. Half-lives were determined as described in Materials and Methods. Samples were taken at the times indicated after rifampin addition or without rifampin. Reprobing was performed with [γ-^{32}P]ATP-labeled oligonucleotide SB767 specific for 5S rRNA. Autoradiograms of the Northern blots are shown. (A) Determination of the BsrF half-life in Spizizen minimal medium without glucose in the presence and absence of Hfq. (B) Determination of the BsrF half-life in TY medium (calculation performed as described above). (C) BsrF binds Hfq. Purified *B. subtilis* Hfq was added to 5′-end-labeled in vitro-synthesized BsrF and incubated for 15 min at 37°C in TMN buffer, and the complex was separated on a 6% native polyacrylamide gel as described previously (18). $t_{1/2}$, half-life.

tetracycline repressor (pWSR2) and the other for constitutive expression of *bsrF* under control of its own promoter (pUCBSR2) in *B. subtilis*. *B. subtilis* Δ*bsrF* strains were transformed with one of these vectors and, as controls, with the empty vectors. The growth curves were identical whether SR2 was overexpressed from multicopy vectors or not (see Fig. S1 in the supplemental material).

These data indicate that neither knockout nor overexpression of *bsrF* affects the growth of *B. subtilis*.

BsrF is long-lived and not stabilized by Hfq. To determine the half-life of BsrF, *B. subtilis* strain DB104 was grown in TY or Spizizen minimal medium at 37°C until the beginning of the stationary growth phase, rifampin (rifampicin) was added to a final concentration of 100 μg/ml, time samples were taken, and total RNA was prepared and subjected to Northern blotting. Quantification of the corresponding gels (Fig. 3) yielded half-lives of BsrF of ~23 min in Spizizen medium and ~55 min in TY medium. Determination of the half-life in CSE minimal medium at an optical density of 2.0 resulted in a value of ~30 min (not shown). The half-life of BsrF in the *hfq* knockout strain DB104 (Δ*hfq::cat*) in Spizizen medium was ~28 min, indicating that BsrF is not stabilized by Hfq (Fig. 3A). However, Fig. 3C shows that BsrF binds Hfq with very low affinity. In summary, we concluded that BsrF is a long-lived RNA.

The BsrF secondary structure includes a long stem-loop with a branched top and a terminator stem-loop. Since com-

puter-predicted RNA structures often deviate from experimentally determined RNA structures (e.g., RNAI/RNAII of pT181 [7]), the secondary structure of BsrF was probed using limited digestion with structure-specific RNases in vitro. BsrF was 5′ end labeled, gel purified, and treated with RNase T$_1$ (which cleaves 3′ of unpaired G residues), RNase T$_2$ (which cleaves unpaired nucleotides with a slight preference for A residues), and RNase V (which cleaves double-stranded or stacked regions). Figure 4 shows the results of the gel analysis and a diagram of the secondary structure derived from the cleavage data. The experimentally determined BsrF structure has in its 5′ half a long stem-loop branched terminally into two small stem-loops and, at the 3′ end, the transcriptional terminator. Two alternative structures for the 5′ terminus can be derived from the experimental data, which might indicate that there is folding equilibrium in vivo.

Of 13 transcription factors analyzed, only CodY had an effect on *bsrF* transcription. A computational search for transcription factor binding sites upstream of the *bsrF* −35 box revealed 13 putative binding sites with up to five mismatches compared with the published consensus sequences (see Fig. S2 in the supplemental material). Knockout strains for all of these factors were used for preparation of chromosomal DNA to construct isogenic *B. subtilis* DB104 knockout strains. DB104 and the isogenic knockout strains were grown under appropriate conditions until logarithmic or stationary growth phase,
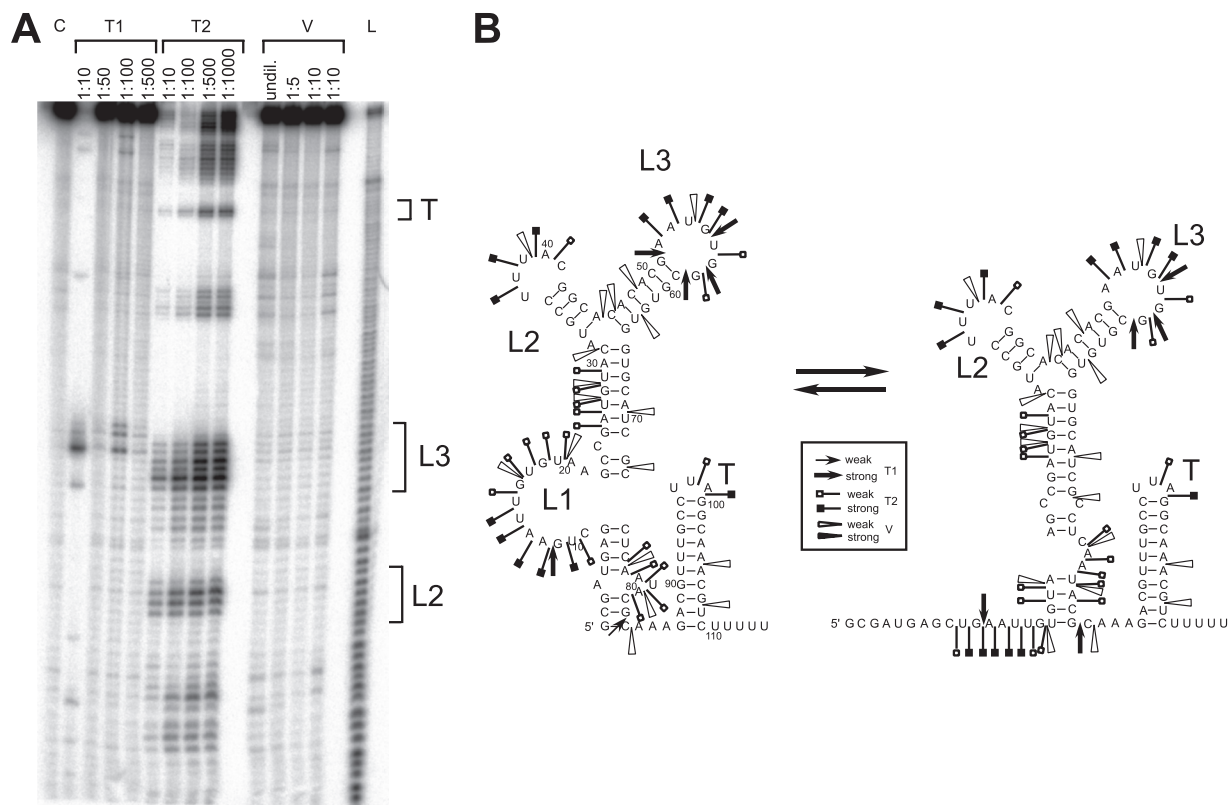
FIG. 4. Secondary structure of BsrF. (A) Secondary structure probing of BsrF with RNases. Purified, 5′-end-labeled BsrF was subjected to limited cleavage with the RNases indicated at the top. The digested RNAs were separated on an 8% denaturing gel. Autoradiograms are shown. The following RNase concentrations used were: RNase T_1, 10^{-2} U/μl (1:50); RNase T_2, 10^{-1} U/μl (1:500); and RNase V_1, 10^{-1} U/μl (1:10). Lane C, control without RNase treatment; lane L, alkaline ladder. undil., undiluted. (B) Proposed secondary structure of BsrF. Two structures consistent with the cleavage data shown in panel A are shown. Major and minor cuts are indicated by symbols. The main stem-loops L1, L2, and L3 and the terminator stem-loop T are indicated.

and total RNA was prepared and subjected to Northern blotting. A difference was observed in only one case. The expression of *bsrF* was increased about twofold in both TY and Spizizen minimal media in the presence of CodY (Fig. 5A). A putative CodY binding site is located 329 bp upstream of the BsrF transcription start site (Fig. 5C). Since Fur, MntR, AhrC, RocR, LevR, and PerR were among the suspected transcription factors, the effects of Fe^{2+}, Mn^{2+}, arginine, fructose, sucrose, and H_2O_2 on the levels of BsrF were analyzed; however, no alteration of the BsrF expression was found. Furthermore, no effect of anaerobic conditions on BsrF expression was detected (data not shown).

BsrF transcription is activated twofold in the presence of glucose, but this effect is independent of both CcpA and CcpN. Transcriptional *bsrF-lacZ* fusions with progressively shorter p_{BsrF} upstream regions containing or lacking the corresponding putative transcription factor binding sites were constructed and integrated into the *amyE* locus of the *B. subtilis* DB104 genome to monitor hypothetical factors influencing *bsrF* expression (Fig. 6B). With pACG6 we observed approximately 1.5- to 2-fold activation of BsrF transcription in Spizizen minimal medium in the presence of glucose, whereas no activation was found with pACG4 lacking a p_{BsrF} upstream sequence (Fig. 6A). No effect of other sugars, like fructose or sucrose, was observed. Since the measured activation is small, a statis-

tical significance test was performed, which confirmed that there was a significant increase in β-galactosidase activity in the presence of glucose (confidence level, 96.5%). To narrow down the *bsrF* upstream region responsible for the glucose effect, pACG13 and pACG12 comprising and lacking a putative CcpA binding site were assayed for β-galactosidase activity, but there were no differences, which is consistent with the absence of an effect of CcpA in the Northern blots (see above). To further narrow down the binding region of a potential glucose-dependent regulator, pACG16 and pACG17 (Fig. 6B) were analyzed. Whereas pACG16 comprising 23 bp upstream of the −35 box of p_{BsrF} still displayed the glucose effect, pACG17 containing 13 bp did not. Since no CcpN binding site was detected upstream of p_{BsrF} and knockout of *ccpN* [strain DB104(Δ*ccpN*::*phleo*) (24)] did not influence BsrF transcription (measured with pACG6), we concluded that the observed glucose effect was independent of both CcpA and CcpN. Furthermore, we assayed the effects of knockouts of CcpC, GlcR, and CggR, which also were found to be not involved in the activation effect of glucose.

CodY activates the transcription of *bsrF* in vivo and in vitro in the presence of BCAA and GTP. Since the results of the Northern blotting showed that CodY had a clear activating effect on the expression of *bsrF* in cells grown in TY and Spizizen media, we analyzed this effect using Northern blots

FIG. 5. CodY affects the amount of BsrF. (A) Effect of CodY on the expression of *bsrF* in TY and Spizizen minimal media. *B. subtilis* DB104 was grown to the OD$_{560}$ indicated, and total RNA was prepared, treated with glyoxal, separated on 2% agarose gels, and subjected to Northern blotting. Autoradiograms of Northern blots are shown. (B) Effect of CodY, glucose, BCAA, and glucose plus BCAA on the expression of *bsrF* in CSE medium. Cultures were grown until the OD$_{600}$ was 0.3 (log phase), and samples were prepared and treated as described above for panel A. An autoradiogram of a Northern blot is shown. (C) Sequence of the *bsrF* upstream region with a putative CodY binding site. The CodY site is enclosed in a box, and the transcription start site is indicated by an underlined G residue and an arrow. −35 and −10 boxes of p$_{BsrF}$ are indicated.

with cells grown in CSE medium with and without BCAA. As shown in Fig. 5B, the amount of BsrF was largest in cells grown in CSE with glucose and BCAA, and under these conditions about threefold more BsrF was observed in the wild-type than in the Δ*codY* strain. In CSE with BCAA but without glucose, slightly less BsrF was detected. To further analyze the BCAA effect, we used a combination of *bsrF-lacZ* transcriptional fusions and in vitro transcription with *B. subtilis* RNA polymerase.

To investigate the influence of BCAA on the expression of *bsrF*, DB104::pACG6 and DB104::pACG6(Δ*codY*::*spc*) were grown in CSE medium with 0.1% glucose in the presence and absence of BCAA (isoleucine, leucine, and valine, 10 mM each). In this experiment, a threefold activating effect of these BCAA in the presence of CodY was observed (Table 2). When isoleucine alone was added instead of all three BCAA, a 2.4-

fold activating effect on BsrF was found, indicating that isoleucine is responsible for 73% of the BCAA effect. By contrast, leucine or valine alone had only an 1.5-fold activating effect. Interestingly, a 1.5-fold difference in β-galactosidase activity between DB104 grown with glucose and DB104 grown without glucose was detectable in the presence of BCAA, but not in their absence. This is in agreement with the observation that glucose has an activating effect in Spizizen medium which also contains BCAA (Fig. 6). There were no differences in the β-galactosidase activities of the *codY* knockout strain grown in CSE medium in the presence of glucose with and without BCAA (Table 2). Since it has been found that CodY binds GTP, a possible effect of GTP on *bsrF* expression was analyzed. To this end, DB104::pACG6 was grown in CSE medium with glucose and BCAA until the optical density at 560 nm (OD$_{560}$)
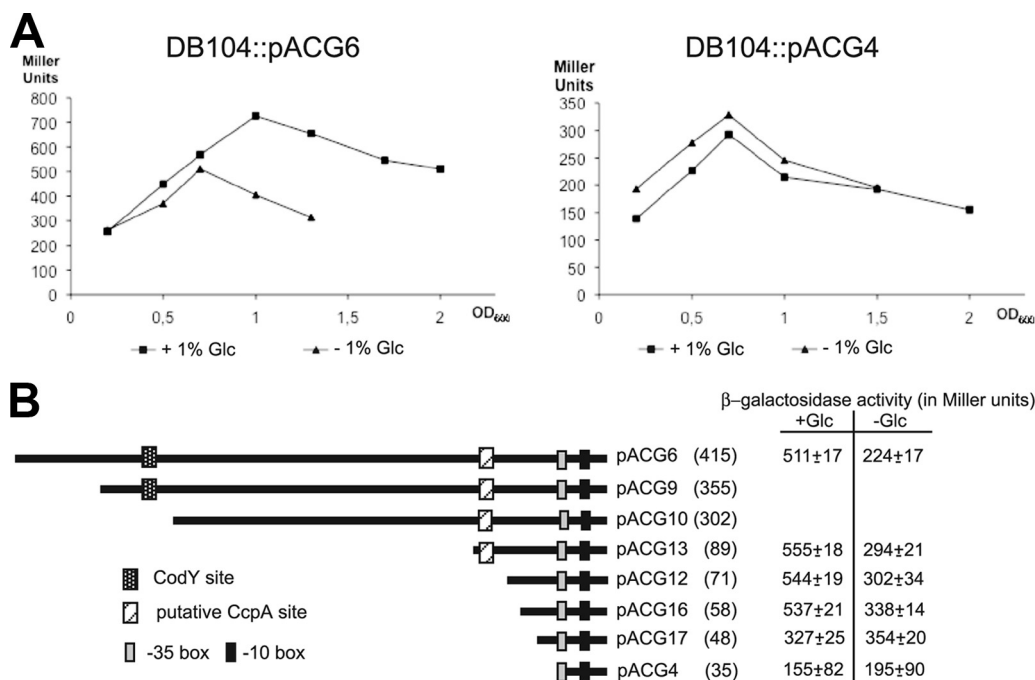
FIG. 6. BsrF transcription is activated in the presence of glucose. (A) Effect of glucose on the *bsrF* expression depending on a sequence upstream of p_{BsrF}. *B. subtilis* strains DB104::pACG6 and DB104::pACG4 were grown in Spizizen medium with and without glucose, and at the OD_{600} indicated, samples were withdrawn and used for β-galactosidase measurement. The data are averages of three independent determinations. (B) Influence of the putative CcpA binding site on the activating effect of glucose on *bsrF* expression. Diagrams of all constructed pACG derivatives are shown. The numbers of base pairs upstream of the *bsrF* transcription start site are indicated in parentheses. The β-galactosidase activities in Spizizen medium with and without glucose at an OD_{600} of 1.3 are indicated on the right. The values are averages for three independent determinations. The −35 and −10 boxes of the *bsrF* promoter, the CodY binding site, and the hypothetical CcpA binding site are indicated.

was 0.3 (logarithmic phase), and samples were removed before and 30 min after addition of mycophenolic acid dissolved in methanol. Mycophenolic acid inhibits IMP dehydrogenase and thus the synthesis of guanine nucleotides, and, therefore, it decreases the cellular GTP pool. Control samples were generated by addition of methanol and incubation for 30 min. Inhibition of GTP synthesis resulted in 1.5-fold-lower β-galactosidase activities in the presence of BCAA, whereas no effect was observed when the cultures were grown in CSE medium without BCAA (Table 2). No influence of GTP was detectable in the Δ*codY* strain.

To confirm our in vivo data in vitro, in vitro transcription experiments with purified native *B. subtilis* RNA polymerase were performed. As shown in Fig. 7, in the absence of CodY, almost no transcript could be detected. By contrast, in the presence of CodY, as well as in the presence CodY and BCAA, a weak transcript that had the expected size (~110 nt) was
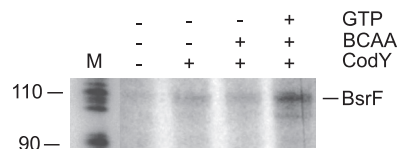
TABLE 2. Influence of BCAA, GTP, and glucose and CodY on BsrF transcription[a]

	β-Galactosidase activity (Miller units)	
Medium	DB104::pACG6	DB104::pACG6 (Δ*codY::spc*)
CSE	305 ± 8	308 ± 5
CSE + BCAA	606 ± 16	318 ± 30
CSE + Glc	303 ± 21	310 ± 25
CSE + Glc + BCAA	909 ± 7	301 ± 33
CSE + Glc + isoleucine	744 ± 10	305 ± 24
CSE + Glc + leucine	445 ± 12	310 ± 15
CSE + Glc + valine	436 ± 15	301 ± 12
CSE + Glc +/− GTP	324 ± 22/312 ± 30	304 ± 10/310 ± 16
CSE + Glc + BCAA +/− GTP	903 ± 50/639 ± 27	308 ± 21/306 ± 27
CSE + Glc +/− methanol	316 ± 15/321 ± 22	ND
CSE + Glc + BCAA +/− methanol	896 ± 43/907 ± 59	ND

[a] All values are averages of at least three independent determinations with five different integrants obtained from cultures grown until the OD_{600} was 0.3 (logarithmic growth phase). The influence of GTP was measured 30 min after addition of mycophenolic acid (a guanine nucleotide synthesis inhibitor) dissolved in methanol (final concentration, 100 μM) or methanol alone to cultures. The concentration of each BCAA (isoleucine, leucine, and valine) added was 10 mM, and the concentration of glucose (Glc) was 0.1 %. ND, not determined. In cases where no glucose was added, the carbon sources in the CSE medium were succinate and glutamate.

FIG. 7. In vitro transcription with *B. subtilis* RNA polymerase. In vitro transcription in the presence or absence of CodY was performed with *B. subtilis* RNA polymerase. BCAA and GTP were added at concentrations of 10 mM and 2 mM, respectively, where indicated. The template was prepared by performing PCR with oligonucleotides SB1233 and SB1064 and comprises the same *bsrF* upstream region as pACG6.

produced, and its intensity increased in the presence of CodY, BCAA, and GTP.

DNase I footprinting confirms the predicted CodY binding site. To delineate the CodY binding site within the *bsrF* upstream region in vitro, DNase I footprinting assays were carried out with increasing CodY concentrations in the presence of 10 mM BCAA and 2 mM GTP. For these experiments, the DNA fragments obtained by PCR with primers SB1233 and SB868 and plasmids pACG6 (wild-type CodY site) and pACG11 (mutated CodY site) were used. As shown in Fig. 8A and B, in the wild-type fragment, one clearly protected region is visible at the predicted CodY binding site. No further CodY sites upstream or downstream of this site were observed. This region was partially protected with 1.4 μM CodY and fully protected with 2.2 μM CodY and is located 329 bp upstream of the *bsrF* transcription start site (Fig. 8D). By contrast, the mutated DNA fragment from pACG11 carrying two C residues at the 3′ end of the poly(A) stretch did not produce any footprint (Fig. 8A). This finding correlates well with the failure of pACG11 to produce any differences in the β-galactosidase assays between DB104 and DB104(Δ*codY*::*spc*) (Fig. 8E). DNase I footprinting performed with an 89-bp DNA fragment generated by annealing two oligonucleotides with the CodY site in its center in the presence or absence of BCAA and/or GTP corroborated the requirement for both BCAA and GTP for the activating effect of CodY (Fig. 8C). Without both effector molecules, no footprint was obtained. An effect of GTP was visible only in the presence of BCAA, whereas BCAA alone had a weak effect.

A mutational analysis reveals the sequence requirements of the CodY binding site for the activating effect on BsrF. To confirm the location of the CodY binding site in vivo, the pACG derivatives pACG9 (25 bp upstream of putative CodY binding site) and pACG10 (13 bp downstream of putative CodY site) were constructed and, along with the previously constructed deletion mutants pACG12, pACG13, and pACG4 (Fig. 6), used for measurement of β-galactosidase activity in DB104 and DB104(Δ*codY*::*spc*) in CSE medium with glucose in the presence and absence of BCAA. The results substantiated the two- to threefold activating effect of CodY on *bsrF* transcription (Fig. 8E). To further analyze the sequence requirements of the CodY binding site, pACG11, pACG15, pACG18, and pACG19 having four different mutations in the predicted CodY binding site were constructed (Fig. 8E). β-Galactosidase measurements for DB104 and DB104(Δ*codY*::*spc*) revealed that mutations in the 3′ terminal A$_7$ tract of the CodY binding site and 3′ terminal two T residues eliminated the ability of CodY to exert its activating effect in the presence of BCAA, whereas a T-G exchange at position 5 did not influence transcription activation by CodY (Fig. 8E).

BsrF is also expressed in *B. amyloliquefaciens* and has an expression pattern similar to that in *B. subtilis*. As shown in Fig. 1D, an sRNA highly homologous to BsrF is encoded in the *B. amyloliquefaciens* genome. Since the promoter elements were identical to those of the *B. subtilis bsrF* gene, we set out to analyze the expression of this predicted sRNA. *B. amyloliquefaciens* FZB42 was grown in TY medium for 10 h, samples were taken at different optical densities, and total RNA was prepared and subjected to Northern blotting with the *B. subtilis* BsrF probe. As shown in Fig. 9, BsrF is expressed in this

species, and, as in *B. subtilis*, the level of BsrF expression is low in early log phase but increases when cells reach late log phase and slightly decreases during stationary growth. Since the upstream region of the *B. amyloliquefaciens bsrF* gene is completely different from that of *B. subtilis*, we searched for a putative CodY binding site. One putative site, which had more mismatches with the consensus than the *B. subtilis* site, was found 100 bp upstream of the −35 box. Strain FZB42 was grown in CSE medium with glucose in the presence and absence of BCAA, samples were removed at an OD_{560} of 1.0, and RNA was prepared and analyzed by Northern blotting. As shown in Fig. 9, an approximately threefold-larger amount of BsrF was observed in the presence of BCAA, suggesting that CodY might be also involved in the expression of *bsrF* in *B. amyloliquefaciens*.

DISCUSSION

The majority of all chromosomally encoded sRNAs are expressed only under specific environmental stress conditions. Many different classes of regulators, including global regulators, have been found to be responsible for this inducible expression. For instance, expression of *E. coli* MicF sRNA is governed by a regulatory network including HU, H-NS, Lrp, OmpR, SoxS, MarA, and Rob (9). *E. coli* RyhB and *B. subtilis* FsrA involved in iron metabolism are regulated by the Fur repressor (11, 28), RprA is regulated by the RcsC/RcsD/RcsB phosphorelay (26), and OmrA and OmrB are regulated by the EnvZ/OmpR two-component system (13). MicA and RybB regulating outer membrane proteins are dependent on the alternative sigma factor σ^E (20, 32, 44, 46) associated with membrane stress. Recently, a novel *Listeria* sRNA that is under the control of the stress sigma factor σ^B was found (31).

Here, we report the properties of a novel sRNA, SR2 (30), identified by our group using the same approach that was used previously for SR1 (24). SR2 was also found independently by Saito et al., who detected six novel sRNAs in intergenic regions of *B. subtilis* and designated BsrF (35). Therefore, the designation BsrF was used in this study. Our sequence alignment revealed a highly homologous sRNA in *B. amyloliquefaciens* (Fig. 1D), and Northern blotting showed that *bsrF* is also expressed in this species with a profile similar to that in *B. subtilis* (Fig. 9). We show here that BsrF is highly expressed in all growth phases and that significant amounts are also present after overnight cultivation (15 h). When cells sporulate, BsrF expression decreases about eightfold (Fig. 2B).

The lack of growth defects upon deletion or constitutive or inducible overexpression of the *bsrF* gene indicates that BsrF, like many other sRNAs, is involved in fine-tuning of gene expression. Surprisingly, the BsrF half-life is very long, and Hfq was found to be not responsible for stabilizing BsrF. Hfq bound BsrF with a very low affinity. Therefore, it is rather unlikely that Hfq promotes the interaction of BsrF with its target(s). To overcome the limitations of a very long-lived sRNA in gene regulation, other factors might cooperate with BsrF to regulate metabolic processes or the stress response.

Furthermore, we demonstrated by using a combination of Northern blotting, *lacZ*-reporter gene fusions, in vitro transcription, and DNase I footprinting that the transcription of BsrF is activated by the global regulator CodY. Thus, the *bsrF*
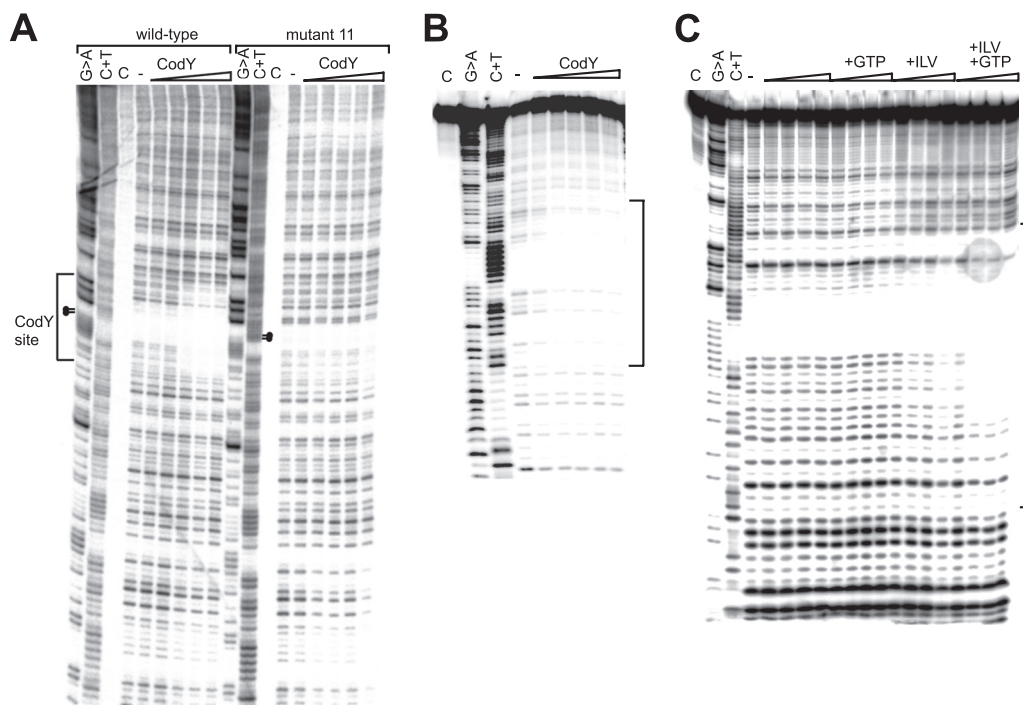
D

```
AACTTATATT ATAATCAAAA AAATTTTGAC AGCTGTTCCT TCTCGTTATT
TTGAATATAA TATTAGTTTT TTTAAAACTG TCGACAAGGA AGAGCAATAA
```

E

		β–galactosidase activity (Miller units)			
		DB104		DB104(ΔcodY::spec)	
		CSE	CSE+BCAA	CSE	CSE+BCAA
AWTWTNCNDAAAATT	Consensus CodY site				
ATAATC<u>A</u>AAAAAATT	pACG6 (wild-type)	303±21	909±7	310±25	301+33
ATAATCAAAAACCTT	pACG11 (mutant 11)	352±32	304±14	350±23	365±31
ATAAGCAAAAAAATT	pACG15 (mutant 15)	305±21	897±15	320±14	310±33
ATAATCAAACCAATT	pACG18 (mutant 18)	324±17	336±20	323±15	324±28
ATAATCAAAAAAAGG	pACG19 (mutant 19)	362±37	359±15	358±32	361±17
ATAATCAAAAAAATT	pACG9 (upstream del)	345±24	776±52	352±24	309±16
CodY site deleted	pACG10	354±32	328±13	368±12	378±32
	pACG13	321±18	344±26	310±30	333±36
	pACG12	314±25	326±12	327±11	342±22
no sequence upstream of -35 box of p$_{BSRF}$	pACG4	189±23	182±20	183±18	179±25

FIG. 8. Interaction of CodY with the *bsrF* promoter region. (A and B) DNase I footprinting analysis of the interaction of CodY and the *bsrF* promoter. DNase I footprinting with increasing amounts of purified CodY-His$_6$ (1.0 μM, 1.4 μM, 1.8 μM, 2.2 μM, and 2.6 μM) (indicated by triangles) was performed in the presence of 2 mM GTP and 10 mM BCAA as described in Materials and Methods. Lane C, control without DNase; lane −, control with DNase but without CodY. The binding site is indicated. (A) Coding strand DNA fragment comprising nt 1 to 176 (Fig. 5C). Dots indicate residues replaced in mutant 11. (B) Noncoding strand (DNA fragment comprising nt 57 to 145 [see Fig. 5C]). (C) Analysis in the presence and absence of CodY, BCAA, and GTP (DNA fragment as in panel B). The triangles indicate increasing amounts of CodY (as described above for panel A). The bracket indicates the region protected by CodY. (D) Sequences on the coding and noncoding strands examined. Protected regions are shaded. The predicted CodY consensus binding site is indicated by bold type. (E) Overview of the mutants with mutations in the CodY binding site. Mutated nucleotides are shaded. The corresponding pACG derivatives and the measured β-galactosidase activities are indicated on the right. Mutated pACG derivatives pACG11, pACG15, pACG18, and pACG19 contain the same region upstream of the CodY site as pACG6, whereas pACG9, pACG10, pACG12, pACG13, and pACG4 contain shortened upstream regions (see Fig. 6). For measurement of β-galactosidase activity, *B. subtilis* strains were grown in CSE medium with 0.1% glucose with or without BCAA (as indicated) until the OD$_{600}$ was 0.3. All of the values are averages of at least three independent determinations with five different integrants.
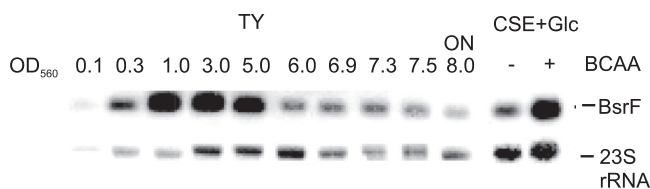
FIG. 9. Expression of the *bsrF* gene in *B. amyloliquefaciens*. *B. amyloliquefaciens* strain FZB42 was grown in TY or CSE medium, and aliquots were removed at hourly intervals at the OD_{560} indicated, immediately frozen in liquid nitrogen, and later used for preparation of total RNA. Northern blotting was performed as described in the legend to Fig. 2 with the same BsrF probe. Autoradiograms of the corresponding gels are shown. ON, overnight cultivation (~15 h). For correction of loading errors, filters were reprobed with [γ-^{32}P]ATP-labeled oligonucleotide SB1319 specific for *B. amyloliquefaciens* 23S rRNA.

gene is the second gene for which an activating effect of CodY has been found (the first gene is *ackA* [38]). The influence of BCAA and GTP on the CodY effect was analyzed both in vivo and in vitro. Whereas BCAA increased the activating effect of CodY about threefold in vivo, the effect of GTP was smaller; in the presence of BCAA, but not in the absence of BCAA, a 1.5-fold increase in the activation effect of CodY was observed in the presence of GTP. The in vitro transcription assay and the DNase I footprinting analysis corroborated the requirement for both GTP and BCAA. This is in contrast to the majority of CodY-regulated operons, including the *ilvB* operon, in which GTP and BCAA were shown to act additively to increase the CodY affinity for DNA and to repress transcription (15). By contrast, relative insensitivity to GTP levels was found for *ackA*, and BCAA alone were observed to be sufficient for the activating effect of CodY (38). Shivers et al. concluded that BCAA and GTP may have independent effects and that promoters differ in their responsiveness to GTP and BCAA pools. This is in good agreement with our observations, which showed that a twofold activating effect of CodY on BsrF also occurred in the stationary phase in TY and Spizizen media, when the sizes of GTP pools are small (Fig. 5A). Interestingly, isoleucine was found to be responsible for 73% of the activating effect of all three BCAA (Table 2). Similar results were obtained for the *ilvB* operon, where isoleucine mimicked the effect of all three BCAA (37). The DNase I footprinting data show that binding of CodY is weak, which may explain the finding that it had only a threefold effect on BsrF transcription in vivo.

In the presence of glucose, BsrF transcription increases about 1.5- to 2-fold, whereas other sugars, like sucrose or fructose, had no effect. Interestingly, the activating effect of glucose found in late log phase (Fig. 6A) was observed only in the presence of BCAA, and none of the known glucose-dependent regulators was responsible for this effect. The region bound by a hypothetical glucose-dependent regulator could be narrowed down to 23 bp upstream of the −35 box of p_{BsrF} (Fig. 6B). Two alternative explanations for the BCAA dependence of this glucose effect can be imagined. On the one hand, a glucose-dependent regulator that binds to a region immediately upstream of p_{BsrF} could cooperate with BCAA-bound CodY, resulting in the threefold activating effect. Such regulatory loops have been found in a number of systems (for a

review, see reference 48). Alternatively, the regulator itself could be subject to transcriptional activation by CodY in the presence of BCAA. For *ackA*, the first gene for which activation of transcription by CodY was demonstrated (38), an interaction of CodY and CcpA was found. However, in this case, the CodY and CcpA binding sites were in close proximity, and CodY bound at two positions, one at positions −61 to −100 upstream of p_{ackA} and the other at positions −20 to 14, and the *cre2* site was found between them. Our DNase I footprinting experiments showed that CodY protects positions −329 to −301 upstream of the BsrF transcriptional start site. Therefore, a regulatory loop involving CodY interacting with the glucose-dependent regulator is conceivable.

Recently, a thorough analysis of all hitherto known CodY binding sites in *B. subtilis* (2) showed broad variation in positions, particularly in the 5′ half of the site, and the consensus sequence 5′-AATTTTCWGAAAATT was derived. Taking into account all of the variations in the original data of Belitsy and Sonenshein (2), we modified this consensus to the more relaxed 5′-AWTWTNCNDAAAATT, which allowed us to find the CodY site upstream of *bsrF*. A mutational analysis of our CodY binding site demonstrated that the A_7 stretch and the two 3′-terminal T residues are the regions most important for CodY binding. By contrast, the T_5-G_5 exchange did not affect CodY activation at p_{BsrF} (Fig. 8E). Attempts to improve the CodY effect on BsrF by mutating the 5′ half of the site toward the consensus, however, failed (not shown.)

Currently, experiments are under way to identify target genes of BsrF. Using Western blotting, we ruled out the possibility that BsrF acts as a *cis*-encoded antisense RNA to regulate *csaA*, which directly overlaps the 3′ end of *bsrF*. The regulation of *bsrF* expression by CodY makes it likely that targets might be discovered that are known to be regulated by CodY but for which no direct CodY binding site has been found, like some of the targets detected in a combined chromatin immunoprecipitation and transcriptome analysis (29). So far, our first microarray analysis revealed a decreased amount of the *cydABCD* mRNA in the Δ*bsrF* strain, suggesting that BsrF might be involved in the regulation of cytochrome synthesis.

REFERENCES

1. **Barrick, J. E., N. Sudarsan, Z. Weinberg, W. L. Ruzzo, and R. R. Breaker.** 2005. 6S RNA is a widespread regulator of eubacterial RNA polymerase that resembles an open promoter. RNA **11**:744–784.
2. **Belitsky, B. R., and A. L. Sonenshein.** 2008. Genetic and biochemical analysis of CodY binding sites in *Bacillus subtilis*. J. Bacteriol. **190**:1224–1236.
3. **Boisset, S., T. Geissmann, E. Huntzinger, P. Fechter, N. Bendridi, M. Possedko, C. Chevalier, A. C. Helfer, Y. Benito, A. Jacquier, C. Gaspin, F. Vandenesch, and P. Romby.** 2007. *Staphylococcus aureus* RNAIII coordinately represses the synthesis of virulence factors and the transcription regulator Rot by an antisense mechanism. Genes Dev. **21**:1353–1366.
4. **Brantl, S.** 1994. The *copR* gene product of plasmid pIP501 acts as a tran-

scriptional repressor at the essential *repR* promotor. Mol. Microbiol. **14:**473–483.

5. **Brantl, S.** 2009. Bacterial chromosome-encoded small regulatory RNAs. Future Microbiol. **4:**85–103.

6. **Brantl, S., B. Nuez, and D. Behnke.** 1992. *In vitro* and *in vivo* analysis of transcription within the replication region of plasmid pIP501. Mol. Gen. Genet. **234:**105–112.

7. **Brantl, S., and E. G. H. Wagner.** 2000. Antisense-RNA mediated transcriptional attenuation: an *in vitro* study of plasmid pT181. Mol. Microbiol. **35:**1469–1482.

8. **Christiansen, J. K., J. S. Nielsen, T. Ebersbach, P. Valentin-Hansen, L. Søgaard-Andersen, and B. H. Kallipolitis.** 2006. Identification of small Hfq-binding RNAs in *Listeria monocytogenes*. RNA **12:**1383–1396.

9. **Delihas, N., and S. Forst.** 2001. MicF: an antisense RNA gene involved in response of *Escherichia coli* to global stress factors. J. Mol. Biol. **313:**1–12.

10. **Faires, N., S. Tobisch, S. Bachem, I. Martin-Verstraete, M. Hecker, and J. Stülke.** 1999. The catabolite control protein CcpA controls ammonium assimilation in *Bacillus subtilis*. J. Mol. Microbiol. Biotechnol. **1:**141–148.

11. **Gaballa, A., H. Antelmann, C. Aguilar, S.-K. Khakh, K.-B. Song, G. T. Smaldone, and J. D. Helmann.** 2008. The *Bacillus subtilis* iron-sparing response is mediated by a Fur-regulated small RNA and three small, basic proteins. Proc. Natl. Acad. Sci. USA **105:**11927–11932.

12. **Geissendörfer, M., and W. Hillen.** 1990. Regulated expression of heterologous genes in *Bacillus subtilis* using the Tn*10* encoded *tet* regulatory elements. Appl. Microbiol. Biotechnol. **33:**657–663.

13. **Guillier, M., S. Gottesman, and G. Storz.** 2006. Modulating the outer membrane with small RNAs. Genes Dev. **20:**2338–2348.

14. **Halfmann, A., M. Kovács, R. Hakenbeck, and R. Brückner.** 2007. Identification of the genes directly controlled by the response regulator CiaR in *Streptococcus pneumoniae*: five out of 15 promoters drive expression of small non-coding RNAs. Mol. Microbiol. **66:**110–126.

15. **Handke, L. D., R. P. Shivers, and A. L. Sonenshein.** 2008. Interaction of *Bacillus subtilis* CodY with GTP. J. Bacteriol. **190:**798–806.

16. **Heidrich, N., and S. Brantl.** 2003. Antisense-RNA mediated transcriptional attenuation: importance of a U-turn loop structure in the target RNA of plasmid pIP501 for efficient inhibition by the antisense RNA. J. Mol. Biol. **333:**917–929.

17. **Heidrich, N., A. Chinali, U. Gerth, and S. Brantl.** 2006. The small untranslated RNA SR1 from the *B. subtilis* genome is involved in the regulation of arginine catabolism. Mol. Microbiol. **62:**520–536.

18. **Heidrich, N., I. Moll, and S. Brantl.** 2007. *In vitro* analysis of the interaction between the small RNA SR1 and its primary target *ahrC* mRNA. Nucleic Acids Res. **35:**331–346.

19. **Hershberg, R., S. Altuvia, and H. Margalit.** 2003. A survey of small RNA-encoding genes in *Escherichia coli*. Nucleic Acids Res. **31:**1813–1820.

20. **Johansen, J., A. A. Rasmussen, M. Overgaard, and P. Valentin-Hansen.** 2006. Conserved small non-coding RNAs that belong to the σ^E regulon: role in down-regulation of outer membrane proteins J. Mol. Biol. **364:**1–8.

21. **Kawamura, F., and R. H. Doi.** 1984. Construction of a *Bacillus subtilis* double mutant deficient in extracellular alkaline and neutral proteases. J. Bacteriol. **160:**442–444.

22. **Kim, H.-J., S.-I. Kim, M. Ratnayake-Lecamwasam, K. Tachikawa, K., A. L. Sonenshein, and M. Strauch.** 2003. Complex regulation of the *Bacillus subtilis* aconitase gene. J. Bacteriol. **185:**1672–1680.

23. **Lee, J. M., S. Zhang, S. Saha, S. Santa Anna, C. Jiang, C., and J. Perkins.** 2001. RNA expression analysis using an antisense *Bacillus subtilis* genome array. J. Bacteriol. **183:**7371–7380.

24. **Licht, A., S. Preis, and S. Brantl.** 2005. Implication of CcpN in the regulation of a novel untranslated RNA (SR1) in *B. subtilis*. Mol. Microbiol. **58:**189–206.

25. **Licht, A., and S. Brantl.** 2006. Transcriptional repressor CcpN from *Bacillus subtilis* compensates asymmetric contact distribution by cooperative binding. J. Mol. Biol. **364:**434–448.

26. **Majdalani, N., D. Hernandez, and S. Gottesman.** 2002. Regulation and mode of action of the second small RNA activator of RpoS translation, RprA. Mol. Microbiol. **46:**813–826.

27. **Mandin, P., F. Repoila, M. Vergassola, T. Geissmann, and P. Cossart.** 2007. Identification of new nonconding RNAs in *Listeria monocytogenes* and prediction of mRNA targets. Nucleic Acids Res. **35:**962–974.

28. **Massé, E., and S. Gottesman.** 2002. A small RNA regulates the expression of genes involved in iron metabolism in *Escherichia coli*. Proc. Natl. Acad. Sci. USA **99:**4620–4625.

29. **Molle, V., Y. Nakaura, R. P. Shivers, H. Yamaguchi, R. Losick, Y. Fujita, and A. L. Sonenshein.** 2003. Additional targets of the *Bacillus subtilis* global regulator CodY identified by chromatin immunoprecipitation and genome-wide transcript analysis. J. Bacteriol. **185:**1911–1922.

30. **Narberhaus, F., and J. Vogel.** 2007. Sensory and regulatory RNAs in prokaryotes: a new German research focus. RNA Biol. **4:**160–164.

31. **Nielsen, J. S., A. S. Olsen, M. Bonde, P. Valentin-Hansen, and B. H. Kallipolitis.** 2008. Identification of a sigma B-dependent small noncoding RNA in *Listeria monocytogenes*. J. Bacteriol. **190:**6264–6270.

32. **Papenfort, K., V. Pfeiffer, F. Mika, S. Lucchini, J. C. D. Hinton, and J. Vogel.** 2006. σ^E-dependent small RNAs of *Salmonella* respond to membrane stress by accelerating global *omp* mRNA decay. Mol. Microbiol. **62:**1674–1688.

33. **Pichon, C., and B. Felden.** 2005. Small RNA genes expressed from *Staphyloccocus aureus* genomic and pathogenicity islands with specific expression among pathogenic strains. Proc. Natl. Acad. Sci. USA **102:**14249–14254.

34. **Ratnayake-Lecamwasam, M., P. Serror, K.-W. Wong, and A. L. Sonenshein.** 2001. *Bacillus subtilis* CodY represses early-stationary phase genes by sensing GTP levels. Genes Dev. **15:**1093–1103.

35. **Saito, S., H. Kakeshita, and K. Nakamura.** 2009. Novel small RNA-encoding genes in the intergenic regions of *Bacillus subtilis*. Gene **428:**2–8.

36. **Sambrook, J., E. F. Fritsch, and T. Maniatis.** 1989. Molecular cloning: a laboratory manual, 2nd ed. Cold Spring Harbor Laboratory Press, Cold Spring Harbor, NY.

37. **Shivers, R. P., and A. L. Sonenshein.** 2004. Activation of the *Bacillus subtilis* global regulator CodY by direct interaction with branched chain amino acids. Mol. Microbiol. **53:**599–611.

38. **Shivers, R. P., S. S. Dineen, and A. L. Sonenshein.** 2006. Positive regulation of *Bacillus subtilis ackA* by CodY and CcpA: establishing a potential hierarchy in carbon flow. Mol. Microbiol. **62:**811–822.

39. **Silvaggi, J. M., J. B. Perkins, and R. Losick.** 2005. Small untranslated RNA antitoxin in *Bacillus subtilis*. J. Bacteriol. **187:**6641–6650.

40. **Silvaggi, J. M., J. B. Perkins, and R. Losick.** 2006. Genes for small, noncoding RNAs under sporulation control in *Bacillus subtilis*. J. Bacteriol. **188:**532–541.

41. **Sonenshein, A. L.** 2005. CodY, a global regulator of stationary phase and virulence in Gram-positive bacteria. Curr. Opin. Microbiol. **8:**203–207.

42. **Storz, G., S. Altuvia, and K. M. Wassarman.** 2005. An abundance of RNA regulators. Annu. Rev. Biochem. **74:**199–217.

43. **Stülke, J., I. Martin-Verstraete, M. Zagorec, M. Rose, A. Klier, and G. Rapoport.** 1997. Induction of the *Bacillus subtilis ptsGHI* operon by glucose is controlled by a novel antiterminator, GlcT. Mol. Microbiol. **25:**65–78.

44. **Thompson, K. M., V. A. Rhodius, and S. Gottesman.** 2007. σ^E regulates and is regulated by a small RNA in *Escherichia coli*. J. Bacteriol. **189:**4243–4256.

45. **Toledo-Arana, A., F. Repoila, and P. Cossart.** 2007. Small noncoding RNAs controlling pathogenesis. Curr. Opin. Microbiol. **10:**182–188.

46. **Udekwu, K., and E. G. H. Wagner.** 2007. Sigma E controls biogenesis of the antisense RNA MicA. Nucleic Acids Res. **35:**1279–1288.

47. **Valentin-Hansen, P., M. Eriksen, and C. Udesen.** 2004. The bacterial Sm-like protein Hfq: a key player in RNA transactions. Mol. Microbiol. **51:**1525–1533.

48. **Xu, H., and T. R. Hoover.** 2001. Transcriptional regulation at a distance in bacteria. Curr. Opin. Microbiol. **4:**138–144.

49. **Zhang, A., K. M. Wassarman, J. Ortega, A. C. Steven, and G. Storz.** 2002. The Sm-like Hfq protein increases OxyS RNA interaction with target mRNAs. Mol. Cell **9:**11–22.